NASA TECHNICAL NOTE

NASA TN D-8315 c.1

NASA TN D-8315

FLIGHT ASSESSMENT OF AN ATMOSPHERIC TURBULENCE MEASUREMENT SYSTEM WITH EMPHASIS ON LONG WAVELENGTHS

Richard H. Rhyne

Langley Research Center
Hampton, Va. 23665

NATIONAL AERONAUTICS AND SPACE ADMINISTRATION • WASHINGTON, D. C. • DECEMBER 1976

1. Report No. NASA TN D-8315	2. Government Accession No.	
4. Title and Subtitle FLIGHT ASSESSMENT OF AN ATMOSPHERIC TURBULENCE MEASUREMENT SYSTEM WITH EMPHASIS ON LONG WAVELENGTHS		5. Report Date December 1976
		6. Performing Organization Code
7. Author(s) Richard H. Rhyne		8. Performing Organization Report No. L-10888
9. Performing Organization Name and Address NASA Langley Research Center Hampton, VA 23665		10. Work Unit No. 743-01-13-01
		11. Contract or Grant No.
12. Sponsoring Agency Name and Address National Aeronautics and Space Administration Washington, DC 20546		13. Type of Report and Period Covered Technical Note
		14. Sponsoring Agency Code
15. Supplementary Notes		

16. Abstract

A flight assessment has been made of a system for measuring the three components of atmospheric turbulence in the frequency range associated with airplane motions (0 to approximately 0.5 Hz). Results of the assessment indicate acceptable accuracy of the resulting time histories and power spectra. Small residual errors at the airplane short-period and Dutch-roll frequencies (0.5 and 0.25 Hz, respectively), as determined from in-flight maneuvers in smooth air, would not be detectable on the power spectra. However, errors of ±0.3 to ±0.6 m/sec (±1 to ±2 ft/sec) at approximately 0.25 Hz can be present in the time history of the lateral turbulence component, particularly at the higher altitudes where airplane yawing motions are large. An assessment of the quantities comprising the vertical turbulence component leads to the conclusion that the vertical component is essentially accurate to zero frequency.

Calculations based upon the performance after each flight of the inertial platform used to measure low-frequency airplane motions indicate that maximum possible linear trend errors on the order of 1.5 to 1.8 m/sec (5 to 6 ft/sec) in 10 min could be present in the time histories of the horizontal turbulence components. A computer experiment indicated that trend errors of this magnitude would affect the power spectral estimate at the lowest frequency (15 240-m (50 000-ft) wavelength) to an appreciable extent only if the turbulence intensity is very light (i.e., turbulence standard deviation (0 to 10 Hz) is about 0.9 m/sec (3 ft/sec)).

17. Key Words (Suggested by Author(s)) Atmospheric turbulence measurement; Turbulence instrumentation; Aircraft instrumentation		18. Distribution Statement Unclassified - Unlimited; Subject Category 05	
19. Security Classif. (of this report) Unclassified	20. Security Classif. (of this page) Unclassified	21. No. of Pages 29	22. Price* $3.75

* For sale by the National Technical Information Service, Springfield, Virginia 22161

FLIGHT ASSESSMENT OF AN ATMOSPHERIC TURBULENCE MEASUREMENT SYSTEM WITH EMPHASIS ON LONG WAVELENGTHS

Richard H. Rhyne
Langley Research Center

SUMMARY

A flight assessment has been made of a system for measuring the three components of atmospheric turbulence in the frequency range associated with airplane motions (0 to approximately 0.5 Hz). Results of the assessment indicate acceptable accuracy of the resulting time histories and power spectra. Small residual errors at the airplane short-period and Dutch-roll frequencies (0.5 and 0.25 Hz, respectively), as determined from in-flight maneuvers in smooth air, would not be detectable on the power spectra. However, errors of ±0.3 to ±0.6 m/sec (±1 to ±2 ft/sec) at approximately 0.25 Hz can be present in the time history of the lateral turbulence component, particularly at the higher altitudes where airplane yawing motions are large. An assessment of the quantities comprising the vertical turbulence component leads to the conclusion that the vertical component is essentially accurate to zero frequency.

Calculations based upon the performance after each flight of the inertial platform used to measure low-frequency airplane motions indicate that maximum possible linear trend errors on the order of 1.5 to 1.8 m/sec (5 to 6 ft/sec) in 10 min could be present in the time histories of the horizontal turbulence components. A computer experiment indicated that trend errors of this magnitude would affect the power spectral estimate at the lowest frequency (15 240-m (50 000-ft) wavelength) to an appreciable extent only if the turbulence intensity is very light (i.e., turbulence standard deviation (0 to 10 Hz) is about 0.9 m/sec (3 ft/sec)).

INTRODUCTION

Power spectral methods for designing airplanes have now become widely accepted. (See refs. 1 and 2.) As larger and more flexible aircraft fly faster, the need for an adequate mathematical model for describing atmospheric turbulence at long wavelengths has become more important since the primary aircraft-response spatial frequency (cycles/m) varies inversely with airspeed. In addition, accurate measurement of atmospheric turbulence over a wide range of wavelength, particularly the long wavelengths, is needed to develop a better understanding of basic atmospheric phenomena that generate turbulence. (See ref. 3.) For these reasons, the Langley Research Center undertook a flight measurement program referred to as Measurement of Atmospheric Turbulence (MAT). The prime objective of the program was to extend power spectra to wavelengths of at least 9100 m (30 000 ft) for a variety of meteorological conditions and a wide range of altitude, with the same instrumentation system employed throughout the investigation. (See ref. 4 for further details.)

Measurement of true gust velocities imposes stringent requirements upon the instrumentation, particularly when the frequency (and wavelength) range is extended over several decades. It is necessary to resolve small fluctuations in flow angles and airspeed with a high degree of accuracy. It is also necessary to determine accurately the inertial motion of the aircraft as it responds to both pilot control inputs and the turbulence field. Since gust velocities are determined from the difference between the flow field measurements and aircraft inertial measurements (which are related), it is necessary that the instrumentation system measure parameters with a negligible phase error. Because of the complex nature of the measurement problem, accuracy can best be assessed by means of flight-test calibrations.

The primary purpose of this report is to present the methods used and results obtained from a flight assessment of the MAT instrumentation and data reduction procedure. This involved taking measurements during pitch-, yaw-, and speed-change maneuvers in smooth air (no turbulence). Special components were developed for the instrumentation system. An inertial navigation system was modified to enable accurate measurement of the three components of gust velocity to a very low frequency. A specially developed airspeed system is sensitive enough for measurements of longitudinal gust velocity up to altitudes of 19 800 m (65 000 ft). (See ref. 5 for further details.)

Low-frequency errors (linear trend type), which cannot be assessed directly by flight-test calibrations, are discussed, and their effect on power spectra is indicated. An artificially generated time history having a known spectral shape is used to illustrate the effect on the spectrum of introducing a known trend into the time history. The maximum trend errors possible in the horizontal velocity measurements from the inertial platform are estimated from postflight platform performance. The effect of these errors on spectra of true gust velocity is assessed for a range of turbulence intensity. A somewhat similar trend error arises from platform measurements of vertical airplane velocity. A data reduction technique is described which removes the trend error from this velocity measurement. The technique is based upon independent pressure altitude meaurements and provides essentially trend-error-free time histories of vertical gust velocity.

SYMBOLS

Measurements and calculations were made in U.S. Customary Units and are presented in both the International System of Units (SI) and U.S. Customary Units.

h_p pressure-derived altitude based on standard atmosphere table (i.e., geopotential altitude as defined in ref. 6), m (ft)

k slope of erroneous linear trend in time history of airplane vertical velocity, also zero error in vertical accelerometer which when integrated produces this trend, m/sec^2 (ft/sec^2)

L scale of turbulence, m (ft)

ℓ horizontal distance between inertial-platform accelerometers and flow-direction sensors, m (ft)

p free-stream static pressure, Pa (psi)

p_t free-stream total pressure, Pa (psi)

q_c impact pressure, $p_t - p$, Pa (psi)

T total duration of run, sec

t time, sec

u_g longitudinal component of gust velocity, positive in direction of flight path, m/sec (ft/sec)

V true airspeed, m/sec (ft/sec)

V_{ax} east-west component of incremental horizontal airplane velocity obtained from inertial platform, with arbitrary zero at instant that data switch is turned on, positive toward east, m/sec (ft/sec)

V_{ay} north-south component of incremental horizontal airplane velocity obtained from inertial platform, with arbitrary zero at instant that data switch is turned on, positive toward north, m/sec (ft/sec)

V_{az} incremental vertical airplane velocity obtained from computer integration of output from vertically oriented accelerometer mounted on inertial-platform stabilized element, positive up, m/sec (ft/sec)

V_x horizontal airplane velocity along inertial-platform east-west axis, positive toward east, m/sec (ft/sec)

V_y horizontal airplane velocity along inertial-platform north-south axis, positive toward north, m/sec (ft/sec)

v_g lateral component of gust velocity, positive toward right wing, m/sec (ft/sec)

w_g vertical component of gust velocity, positive up, m/sec (ft/sec)

α angle of attack, positive with flow-vane trailing edge up, rad

β angle of sideslip, positive with flow-vane trailing edge toward right wing, rad

Δa_z incremental vertical acceleration obtained from inertial platform with reference to 1g level flight, positive up, m/sec^2 (ft/sec^2)

Δh_p incremental pressure-derived altitude with reference to value at beginning of run (see definition of h_p), positive when altitude increases, m (ft)

Δp incremental free-stream static pressure with reference to value at beginning of run, Pa (psi)

Δp_t incremental free-stream total pressure with reference to value at beginning of run, Pa (psi)

Δq_c incremental impact pressure with reference to value at beginning of run, Pa (psi)

$\Delta\psi$ incremental sensitive airplane heading with arbitrary zero at instant that data switch is turned on, measured in horizontal plane, positive with nose right, rad

θ pitch attitude, measured in vertical plane, positive with nose up, rad

$\dot{\theta}$ pitch rate measured by body-mounted pitch-rate transducer, positive with nose going up, rad/sec

λ wavelength, or distance per cycle, m (ft)

σ standard deviation, m/sec (ft/sec)

ϕ roll attitude of airplane with reference to horizontal, positive with right wing down, rad

ψ airplane heading, measured in a horizontal plane clockwise from grid north,[1] always positive, deg or rad

$\dot{\psi}$ yaw rate measured by body-mounted yaw-rate transducer, positive with nose going right, rad/sec

A bar over a symbol indicates average over the entire run.

A caret over a symbol indicates that the quantity is given with respect to the mean for the entire run; that is, the mean has been subtracted.

---

[1]Grid north is true north at the platform alinement location, but as the platform moves east or west from its initial alinement point, its north-south axis is not torqued to point at true north but remains parallel to a vertical plane through the meridian at which it was alined. (The north-south and east-west axes are torqued to be perpendicular to the local vertical at all times, however.) For all practical purposes the inertial-platform axis system can be assumed to be alined with true north, considering the latitudes of operation and the east-west distances flown in the MAT project.

BACKGROUND

The method of measuring true gust velocities from a flow-vane instrumented aircraft was developed simultaneously by both NACA and Cornell Aeronautical Laboratory in 1954 (refs. 7 and 8). The velocities so obtained were the true motions of the air particles relative to an Earth-fixed axis system. The axis system was generally alined with the mean flight path of the aircraft, with gust velocity components perpendicular to the mean path of the vehicle obtained in a vertical plane and, in later investigations, in a horizontal plane. Power spectral procedures for the calculation of airplane response to turbulence had been developed prior to this time (ref. 9), and the newly developed method of measuring true turbulence input found ready application. Results of the measurements of true gust velocities were immediately shown to be most useful in the form of power spectra, as indicated in references 7 and 8.

Although power spectral measurements of true gust velocity from a variety of meteorological conditions and for range of altitude were desirable, extensive recording and combining of the rather large number of corrective airplane motion measurements required for data processing was impractical at the time. The method was well established, however, and its basics are still in use today.

As digital methods for recording large numbers of data channels on magnetic tape were developed and modern high-speed computers for data processing became available, additional power spectral turbulence measurement programs were undertaken. (See refs. 10 to 12, for example.) Results from these programs have, in general, led to the conclusion that the Von Karman mathematical model of atmospheric turbulence (described in ref. 13) is valid for the slope of the power spectrum (-5/3) at spatial frequencies (inverse wavelength) above about 3.3×10^{-3} cycle/m (10^{-3} cycle/ft) for a number of meteorological conditions. Considerable uncertainty still exists as to the appropriate value of L, the so-called integral scale value, and even to the applicability of the Von Karman model at lower values of spatial frequency (longer wavelengths). Experimental evidence at longer wavelengths has been lacking because drift-free airplane attitude and velocity measurements and long sample lengths required to obtain statistical reliability of the power spectral estimates (which must be made at smaller frequency intervals) were difficult to obtain. Also selection of appropriate filtering and processing techniques is required.

CALCULATION OF GUST VELOCITY COMPONENTS

Time histories of the three gust velocity components were determined in the data reduction process from the following equations, which also indicate the measurements required:

Longitudinal component

$$u_g = (-\hat{V}) + (\hat{V}_{ax} \sin \bar{\psi} + \hat{V}_{ay} \cos \bar{\psi}) \tag{1}$$

Lateral component

$$v_g = (V\hat{\beta}) + (-V\,\widehat{\Delta\psi} + \hat{V}_{ax}\cos\bar{\psi} - \hat{V}_{ay}\sin\bar{\psi} + \ell\hat{\dot{\psi}} + V\hat{\alpha}\phi) \tag{2}$$

Vertical component

$$w_g = (V\hat{\alpha}) + (-V\hat{\theta} + \hat{V}_{az} + \ell\hat{\dot{\theta}} - V\hat{\beta}\phi) \tag{3}$$

The first term on the right side of each equation represents airflow measurements. Subsequent terms represent airplane motion corrections. The equations are basically those given and discussed in reference 13, with modifications to incorporate the inertial platform measurements directly. (These modifications, along with a more detailed derivation of the equations can be found in ref. 14.) The assumptions of reference 13 and the present study are that (1) all disturbances are small enough to allow use of the angle in radians in place of the sine or tangent of the angle, (2) structural flexure between the inertial-platform measuring station and the airflow measurement location on the nose boom is negligible, and (3) induced upwash effects on the flow-vane indications are negligible.

The horizontal axes for equations (1) to (3) are fixed by the mean heading angle $\bar{\psi}$ for each separate run. In calculation of each gust velocity component, fluctuations are given with respect to an arbitrary mean value. In the case of the longitudinal component u_g, for example, $\hat{V}$ is true airspeed with respect to the mean true airspeed for the run, $\hat{V}_{ax}$ is incremental inertial velocity along the platform's east-west axis with mean removed, and $\hat{V}_{ay}$ is incremental inertial velocity along the platform's north-south axis with mean removed. The only airplane motion measurements which do not come from the inertial platform are $\dot{\psi}$ and $\dot{\theta}$, which are obtained from body-mounted yaw-rate and pitch-rate transducers, respectively. The distance ℓ associated with these measurements is the distance between the platform-mounted accelerometers and the flow-direction sensors. The terms involving ℓ account for the difference in linear velocity between the platform measuring station and the $\hat{\alpha}$ and $\hat{\beta}$ measuring station due to yaw rate and pitch rate, and are generally quite small. The misalinement between the airplane body axis and the horizontal platform axis is thus ignored in this case. However, the $V\hat{\alpha}\phi$ term in equation (2) and the $V\hat{\beta}\phi$ term in equation (3) are cross terms which do account for the angular misalinement between the two axis systems with regard to attitude. These second-order terms are quite small and can be ignored in most cases.

INSTRUMENTATION AND HARDWARE

Since the primary purpose of the MAT project is to obtain accurate measurements of gust velocity to very low frequencies (long wavelengths), an inertial navigation system modified for this application measures airplane motions. (See ref. 5 for details of instrumentation.) The airplane motions are then applied as corrections to the airflow measurements to obtain gust velocity.

The airflow measurements are made on a nose boom extending well ahead of the airplane to minimize the effects of the airplane flow field. The nose boom can be seen in figure 1, a photograph of the MAT project airplane. Figure 2 is a close-up photograph of the special pitot-static head, with balsa flow-direction vanes installed. The flow vanes are located 2.01 m (6.59 ft) ahead of the original nose, or 8.37 m (27.45 ft) ahead of the wing leading edge. To insure that deflections in the structure between the flow vanes and the inertial platform cannot cause angular and/or vibratory effects which cannot be accounted for, it is desirable to have a nose boom whose natural frequency is 10 to 12 Hz or greater. The tapered construction of the present installation resulted in a very stiff, lightweight nose boom, with a natural frequency of about 25 Hz when measured on the airplane with pitot-static head and flow vanes installed.

Details of the individual measurement channels, including the associated electronic equipment, method of recording, frequency response, range, and estimated accuracies are given in reference 5. The sensitive airspeed system developed for use in the MAT project is described herein because of its importance in obtaining the longitudinal turbulence component. The principle of operation is first to obtain the steady-state true airspeed at the beginning of each data run by means of conventional measurements of impact and static pressure, and then to measure incremental pressures by means of separate auxiliary transducers during the remainder of the run. These auxiliary transducers then must cover only the range of fluctuations caused by the turbulence and by the pilot in controlling the airplane, and thus the required pressure range is considerably reduced, with a resulting increase in accuracy and resolution. The method of operation is illustrated by the schematic drawing in figure 3. Valves A and B are ordinarily open during climb and speed changing so that changing pressures are equalized on both sides of the sensitive transducers (shown below valves A and B) and in the chambers shown. At the beginning of a data run, the pilot's data switch activates solenoids which close valves A and B to "lock" reference pressures which exist at that instant in the volume chambers. These volume chambers are heavily insulated and thermostatically controlled so that thermal drifts do not cause detectable pressure changes on the sensitive transducers during the data-recording interval. Once valves A and B are closed, incremental total pressure and incremental static pressure are recorded for the remainder of the run in addition to coarse-resolution impact pressure and free-stream static pressure.

Although the pilot maintains a reasonably horizontal flight path during the run, small changes in altitude would contaminate the measurements of Δp_t (and thus the measurements of incremental true airspeed) at a low frequency if not removed in the data reduction by use of the incremental static pressure recording. In other words, what is needed for obtaining true airspeed fluctuations is actually Δq_c, or incremental impact pressure (equal to $\Delta p_t - \Delta p$), which is readily obtained in the postflight data reduction. The dynamic requirements of the static pressure measurements are not stringent since the airplane does not change altitude very rapidly. In order to improve the dynamics of the total pressure measurement, interchangeable restrictor orifices are installed at the front of the boom according to the anticipated altitude range for the particular mission. Their effect is to compensate for changes in damping (of the air column plumbing system) due to air temperature changes.

Although not indicated in figure 3, there are actually two pressure transducers for each of the two incremental pressure measurements, one having a recording range of ±1720 Pa (±0.25 psi), and the other a range of ±690 Pa (±0.1 psi). The more sensitive of the transducers was allowed to go off scale at the lower altitudes where its sensitivity was not needed, but it remained on scale during use at the higher altitudes. After the first few flights, it was found that the pilot even had difficulty in keeping the ±1720-Pa (±0.25-psi) range Δp_t transducer on scale in the rougher turbulence at low altitude. (As the airplane climbs because of a slight nose-up condition, the airspeed tends to decrease; and the increasing altitude and the decreasing speed couple to reduce the total pressure; the opposite effect, of course, takes place for a slight nose-down out-of-trim condition.) This problem was solved by combining the Δp_t and Δp transducer signals electrically so that they were subtracted onboard, rather than in the postflight data reduction, to obtain Δq_c. The ±1720-Pa (±0.25-psi) recording range for Δq_c then proved to be adequate since the effect of the altitude change was no longer present in this quantity. It should be pointed out that the linear range of the individual Δp_t and Δp transducers was more than ±3450 Pa (±0.5 psi), so that a transducer linear range exceedance was not expected to occur. As a precaution, Δp_t was recorded and monitored over a range of ±3450 Pa (±0.5 psi). In addition, the Δp pressures were recorded separately, as before, for use in obtaining fine-resolution altitude changes during the runs.

ASSESSMENT OF MAT SYSTEM BY IN-FLIGHT MANEUVERS

Pilot-induced maneuvers in smooth air provide a good practical means of checking the overall instrumentation and the data reduction procedure. The quantities recorded during the maneuvers are simply inserted into equations (1), (2), and (3). Time histories of the resulting turbulence components u_g, v_g, and w_g are expected to remain nearly zero during the maneuver. The maneuvers, of course, must be made in very calm air or in a sufficiently large uniform moving air mass so that appreciable changes in air movement do not occur during the maneuver. In practice, exactly zero gust velocities are seldom attained because of the stringent nature of the test. It should be pointed out that the relative amplitude and phase of the various motions induced by the pilot are not exactly the same as those caused by actual turbulence. For example, to generate appreciable vertical airplane accelerations and associated vertical airplane velocities (the $\hat{V}_{az}$ term) in smooth air maneuvers, the pilot must induce by means of elevator control much larger pitch attitude changes (the $V\hat{\theta}$ term) than are present during turbulence flight. In addition, the $V\hat{\theta}$ oscillation caused by the maneuver strongly correlates with the $\hat{V}_{az}$ oscillation; this is not the case for flight in turbulence. The technique employed by the pilot in rough air can also influence the magnitude of some motions to a considerable extent. The pilot's instructions for rough air flight are (1) to maintain airplane attitudes reasonably centered within the available recording range by means of gradual control movements (special pilot displays connected to the instrumentation provided assistance in this task) and (2) to maintain altitude and airspeed as close as practical to the altitude and airspeed at the beginning of the run. No special attempt is made by the pilot to control the short-period and Dutch-roll motions of the airplane.

Pitching Oscillation

Figure 4 presents the result of a typical pitching oscillation maneuver at an altitude of 7990 m (26 200 ft). The terms in equation (3) for w_g are plotted separately with the same units and scale factor so that their relative amplitude and phase can be easily observed. The frequency of the motions is about 0.5 Hz, which approximates the airplane's short-period stability mode which is excited in rough air. The amplitude of the 0.5-Hz pitch attitude oscillation (the $V\hat{\theta}$ term) is considerably greater here than that experienced in rough air at 0.5 Hz, although the total range covered (about 17.4 m/sec (57 ft/sec)), including the gradual nose-down change in trim, is not too unusual for a 10-min turbulence run. The total range of $V\hat{\theta}$ in rough air is mainly a function of the pilot's skill and attention in controlling the airplane. The $\ell\dot{\hat{\theta}}$ term is also several times larger than that usually experienced in rough air. The computed vertical gust velocity w_g is shown at the bottom of figure 4 and should of course be zero, instead of the ±0.6 to ±0.9 m/sec (±2 to ±3 ft/sec) shown.

The residual gust velocity shown in figure 4 is not considered excessive in view of the rather large amplitude of the induced pitching motions. It is seen that the lower frequency component of the maneuver (as evidenced by the downward trend of the $V\hat{\theta}$ oscillations) is completely counteracted by the downward trend of $\hat{V}_{az}$ as can be seen by the absence of any low-frequency trend in w_g.

At least one-half of the residual gust velocity oscillation can be accounted for by the upwash created at the flow-vane measuring station by the flow field of the airplane. Physically, the flow field around the oscillating wing extends upstream far enough to cause the vane measuring incremental angle-of-attack $\hat{\alpha}$ to read high. Calculations for the MAT airplane under average flight conditions, based on the method of reference 15, give an induced upwash factor of about 10 percent of the angle of attack. Close inspection of figure 4 indicates that the residual gust velocity is nearly in phase with $V\hat{\alpha}$ (w_g appears to be lagging slightly), and that a 10-percent amplitude reduction in $\hat{\alpha}$ would reduce the gust velocity oscillation considerably. However, this simple correction will not suffice for turbulence measurements, since it is based on quasi-static flow effects about the wing. Penetration of the turbulence flow field by the airplane, the dynamics of flow buildup about the wing due to turbulence, and propagation forward to the flow vane make such an upwash correction considerably more complicated. Such corrections have generally been ignored in the past. Some justification for not attempting such a correction here is the fact that a "noise hump" at 0.5 Hz has not been discernible on the power spectra obtained to date with the MAT instrumentation. The lack of such a power peak can probably be attributed to the relatively low amplitude of the short-period motions of the MAT airplane. (Generally, the amplitude of pitching motions at 0.5 Hz is not greater than about one-third that shown in fig. 4.)

Yawing Oscillation

Figure 5 presents results from a yaw oscillation made in smooth air at an altitude of about 4660 m (15 300 ft). The terms of equation (2) are plotted in the same way as in figure 4. The pilot forced the first cycle of the oscillation by rudder movement and then allowed the motion to decay naturally. The rather slow decay rate is evidence of the airplane's lack of damping in yaw, which is even more pronounced at higher altitudes. The amplitude of the various terms is quite similar to that caused by actual turbulence. It might be noted that the relative size of the two platform horizontal velocity terms (i.e., $\hat{V}_{ax} \cos \bar{\psi}$ and $\hat{V}_{ay} \sin \bar{\psi}$) during an overall heading change (which occurs here) depends upon the airplane's mean heading $\bar{\psi}$. In the example of figure 5, it is apparent that the airplane is on a predominantly north-south heading, since $\hat{V}_{ax} \cos \bar{\psi}$ changes with $\hat{\Delta\psi}$ with practically no change occurring in $\hat{V}_{ay} \sin \bar{\psi}$. On a 45° mean heading, both terms would be affected equally.

The results of the yawing oscillation are more important than the pitch results, since airplane yawing motions of approximately this amplitude are constantly present in turbulence of moderate intensity. In figure 5, lateral gust velocity v_g is ±0.3 to ±0.6 m/sec (±1 to ±2 ft/sec). This erroneous oscillation at a frequency of about 0.25 Hz (approximately the Dutch-roll frequency of the airplane) will probably be discernible in the time history of lateral gust velcity. The size of a resulting hump in the power spectrum at 0.25 Hz can be estimated by assuming that the noise is a sine wave with peak amplitude of ±0.6 m/sec (±2 ft/sec). The mean square, or power spectral area contribution, would thus be

$$\sigma^2_{\text{sine wave}} = \left(\frac{\text{Amplitude}}{\sqrt{2}}\right)^2$$

When the amplitude is ±0.6 m/sec (±2 ft/sec), the mean square would be 0.18 m²/sec² (2 ft²/sec²). If moderate intensity turbulence is assumed to have a standard deviation σ of 3 m/sec (10 ft/sec), the total area under the power spectrum σ^2 would be 9 m²/sec² (100 ft²/sec²). The percentage area contribution of the noise arising from the yawing oscillation would thus be only 2 percent and would probably be obscured by normal fluctuations of the power estimates.

The reason for the ±0.3 to ±0.6 m/sec (±1 to ±2 ft/sec) residual gust velocity obtained in the yawing maneuver can probably be attributed to a small phase difference between the $\hat{\Delta\psi}$ and $\hat{\beta}$ time histories which has not been accounted for. It is noted that the overall heading change (caused by the pilot's first rudder oscillation being slightly unsymmetrical) is compensated for quite adequately by the $\hat{V}_{ax} \cos \bar{\psi}$ term, so that zero gust velocity is effectively maintained at this lower frequency.

Speed Change

On one or two occasions a speed-change maneuver was performed as a matter of interest and to serve as a direct check on the true airspeed measuring capability. (Pitching and yawing maneuvers were generally performed in smooth air on every flight and were considered an adequate overall check of the instrumentation.) In figure 6 the terms of equation (1) are plotted during a speed-change maneuver. Since it was made on an almost exact east-west heading, only the $\hat{V}_{ax} \sin \bar{\psi}$ term is active. A very small amount of turbulence is indicated during this run by the meager high-frequency content of the incremental true airspeed ($\hat{V}$ term), and of the resulting gust velocity component u_g. The amplitude of the speed-change maneuver could not have been much larger at this altitude without exceeding the ±1720-Pa (±0.25-psi) recording range of Δq_c.

The results of the speed-change maneuver shown in figure 6 primarily serve to show that the special measurements and data reduction procedures for obtaining incremental true airspeed are correct. Such a maneuver is not itself representative of motions encountered in turbulence. Possible error in the longitudinal gust component which correlates with the maneuver is not apparent; however, very small errors could be masked by the very low-intensity turbulence present. The steep inertial speed change ($\hat{V}_{ax} \sin \bar{\psi}$) was caused by the pilot applying an abrupt power change. Changes of this steepness do not ordinarily occur during the turbulence runs since power settings are changed only slightly, if at all. Changes of this nature in true airspeed $\hat{V}$ might occur because of wind shear or mountain wave effects, however. Observation of the motion records in turbulence indicates that the airplane itself does not respond appreciably to air motions in the longitudinal direction until somewhat longer wavelengths are reached.

ASSESSMENT OF VERY LOW-FREQUENCY AND TREND ERRORS

Although higher frequency system errors can be assessed by means of in-flight maneuvers, extremely low-frequency drifts, or trend errors, cannot be easily determined from such tests. The tests would need to be of at least 10-min duration and would thus cover a distance of 110 km (60 n. mi.) or more. Even on very calm days, the atmosphere is in continual motion, and one probably could not expect to travel that far without encountering changing air motions of a minimum of 1.5 to 3.0 m/sec (5 to 10 ft/sec). It is apparent, therefore, that low-frequency trend errors cannot be readily distinguished unless they are of a systematic nature or of appreciable magnitude.

Almost all of the individual measurements from the MAT system were adequately assessed for very low-frequency and trend errors by ground-based procedures. For example, the flow-direction vanes were locked in a fixed position by their calibration jigs, and their electronic outputs observed for stability over long periods of time. Likewise the pressure measurements were observed for possible trends caused by thermal drifts and other instabilities. Three measurements, the airplane velocities obtained from the inertial platform, can only be assessed for low-frequency errors in an indirect manner. These measurements are very important in determining the low-frequency part of the turbulence power spectra, and are discussed in the following sections.

Vertical Airplane Velocity

Since inertial platform systems are not generally designed to provide navigation information in a vertical plane, special vertical velocity signals extracted from such systems may not be reliable to zero frequency, and consequently, they can have undesirable trend errors. The basic difficulty is that the vertically oriented platform-mounted accelerometer (from which the vertical velocity information must be derived) is susceptible to changing Coriolis forces from run to run, as a result of changing ground tracks with respect to the Earth's rotation. This effect is not compensated for by the system's computer. Another effect is the change in the Earth's gravity constant with altitude. This effect is largely removed by a special compensation provided in the MAT instrumentation which generates an electrical signal proportional to altitude from a static pressure measurement. The result of either or both of these effects is an apparent shift in the zero of the vertical accelerometer from run to run, which when integrated produces an unknown linear trend in the derived vertical airplane velocity, and, in turn, in the vertical turbulence component. (The accelerometer zero for any one run, although not precisely known, is quite stable since the pilot maintains the heading and altitude within fairly close limits.)

One way of overcoming this difficulty is to integrate the accelerometer output in the postflight data reduction rather than to utilize onboard electronic integration. Points along the time history where the vertical airplane velocity is estimated to be zero are chosen to start and stop the integration. These start and stop times are chosen by inspection of the time history of the sensitive incremental static pressure Δp (an altitude indication); that is, points are chosen where the slope of the time history is zero. A mean for the accelerometer output for this time range is then determined on the computer. When the mean (which is determined to a large number of digits and not limited to the resolution of the individual acceleration readings) is subtracted and the integration performed, the resulting velocity time history has thus been forced to start and stop at zero.

This procedure has limitations however. It is not easily automated into the data reduction process, and exact points along the time history where zero vertical velocity occurs are hard to determine because of a certain amount of noise present in the time history of the sensitive static pressure. (This relatively high-frequency noise results from cross flow over the static port locations on the pitot-static head, particularly in severe turbulence.) Another disadvantage is that zero vertical velocity points may not occur at convenient locations near each end of the time history, and, in fact, for the shorter pitch and yaw maneuvers, they may not occur at all.

A more efficient procedure, which accomplishes the same result but with greater accuracy and no limitation on the starting and stopping points, is now described. The basis for the procedure is the fact that when an erroneous trend of slope k is integrated over total time T (with mean removed), a parabolic error with a maximum value at $T/2$ of $-kT^2/8$ results. The maximum error at $T/2$ is determined experimentally in the present case by double integration of the platform-mounted accelerometer output to obtain a time history of inertial displacement. This displacement is then compared with the time history of the pressure-derived altitude. An illustrative sketch of the procedure is as follows:

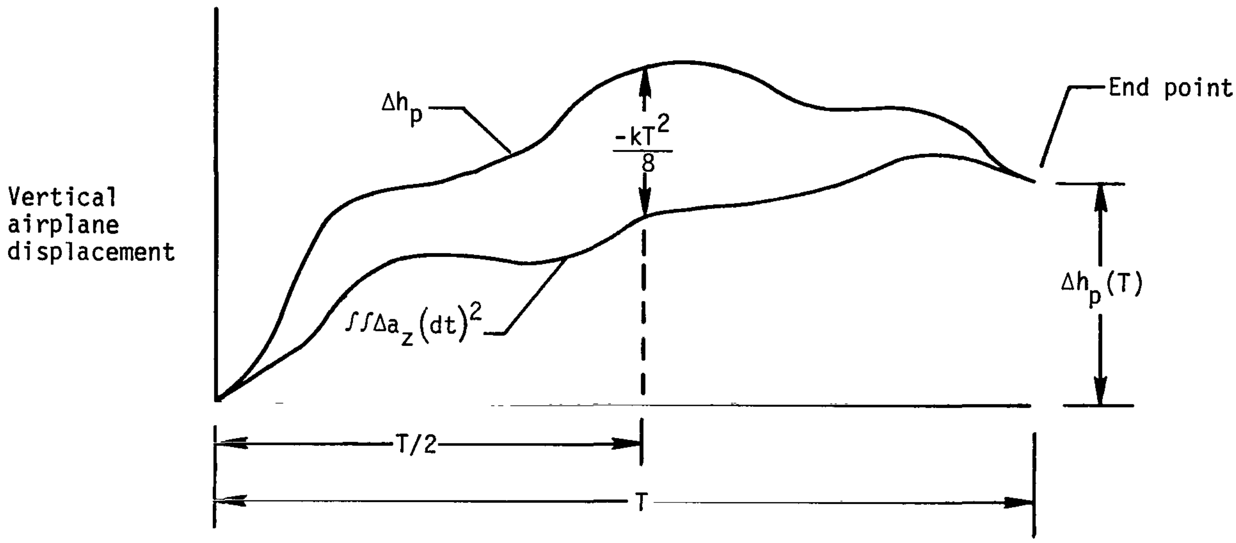

It should be noted that the end point of the time history of $\int\int \Delta a_z(dt)^2$ has been forced to agree with the time history of Δh_p at the end of the run by an adjustment to the initial condition of the first integration; that is, the last integration is then $\int(V_{az} - \overline{V}_{az} + C)dt$, where $C = \Delta h_p(T)/T$. The whole procedure has been automated in the data reduction process. The displacement error at the midpoint of the run is obtained by averaging over ±1/2 sec to minimize possible effects of the previously mentioned high-frequency noise on the time history of sensitive pressure altitude. The value of k obtained is applied as a detrend slope correction to the vertical airplane velocity obtained from the first integration.

As a check on the overall procedure, the vertical airplane velocity V_{az} was again integrated after the detrending procedure and was compared with the pressure altitude. The resulting time histories, which are for a 12-min turbulence run at an altitude of 13 100 m (43 000 ft), are shown in figure 7. This particular turbulence run is of interest because of the unusually large altitude excursions. The amplitude of the excursions obtained by the two methods agrees quite well. Certainly all systematic parabolic error between the two quantities has been eliminated. Thus, the airplane vertical velocity measurements must be essentially accurate to zero frequency. The cause of the very slight discrepancy between the two quantities near the beginning of the run is not known. Other measurements indicate that a large wind shear (decrease in head wind) was encountered at about that time and caused the pilot's indicated airspeed to drop. Such a drop in airspeed might have caused him to put the airplane's nose down, causing the 300-m (1000-ft) drop in altitude. Altitude oscillations generally of smaller amplitude than the first oscillation of figure 7 are quite often present. These are the result of the airplane's phugoid or long-period mode. Some pressure noise (discussed previously) caused by the turbulence can be seen about 5 min after the beginning of the run, and again at 8 min.

Horizontal Airplane Velocity (V_{ax} and V_{ay})

The accuracy of the fine-resolution platform incremental velocity measurements V_{ax} and V_{ay} is dependent upon the general performance of the inertial platform and its computer system. As indicated previously, the accuracy of these measurements at very low frequencies cannot be readily assessed to the necessary precision by in-flight measurements. A good indication of the platform's performance and of the maximum probable errors in these quantities is obtained by monitoring the velocity readouts after each flight while the platform system is still operating. The velocities theoretically should be zero at this time, since the airplane is motionless. Errors have built up during the flight however, and cause a very small ocillation in the stabilized element with a period of 84.4 min. This 84.4-min oscillation is the result of what is referred to as Schuler tuning of the platform-computer system. (See ref. 16.) The amplitude of this Schuler oscillation is not damped and generally does not decrease during a flight but continues to build up with time as errors occur in the system (ref. 16). The platform oscillation is too small to be detectable in the pitch and roll measurements, but is observable in the velocity measurements because of the Earth's gravity vector affecting the platform-mounted north-south and east-west accelerometers.

Since the amplitude of the inertial platform's Schuler oscillation is judged to be a good indication of the maximum possible error which could have occurred during that particular flight, the Schuler oscillation was monitored after each flight by making 84-min recordings of velocity. These velocity time histories were almost perfect sine waves (of 84-min period) but were sometimes offset from zero by an overall trend or "ramp effect." This ramp effect would only be of concern with regard to the coarse-resolution absolute velocities V_x and V_y and never was of sufficient slope to produce a noticeable effect on the fine-resolution incremental velocities used to obtain the turbulence time histories. (The ramp effect was generally never as large as the Schuler oscillation, even when the inertial system had been in its flight mode for 4 or 5 hr.)

The magnitude of the postflight Schuler oscillation for all the flights was generally between 3 and 5 m/sec (10 and 15 ft/sec) from peak to peak. For the purpose of estimating the maximum possible errors in V_{ax} and V_{ay} during turbulence runs (and therefore in the turbulence time histories), it is assumed that the in-flight errors are sine waves having the 84.4-min period and the postflight Schuler amplitude. It is also assumed that the mean heading $\bar{\psi}$ is such that the Schuler error is reflected in the gust component in the worst possible manner; that is, that either $\sin \bar{\psi} = 1$, or $\cos \bar{\psi} = 1$. It is recognized that the in-flight errors are not necessarily smooth sine waves and that error in the inertial system may not build up in a smooth fashion over the duration of the flight. It is believed however, that calculations based on these assumptions provide an indication of the maximum possible error in any one run. A 10-min turbulence run would have the maximum error, or the maximum effect of trend slope, if it occurred at the position on the Schuler error cycle shown in the following sketch, that is, 5 min on either side of the zero crossing:

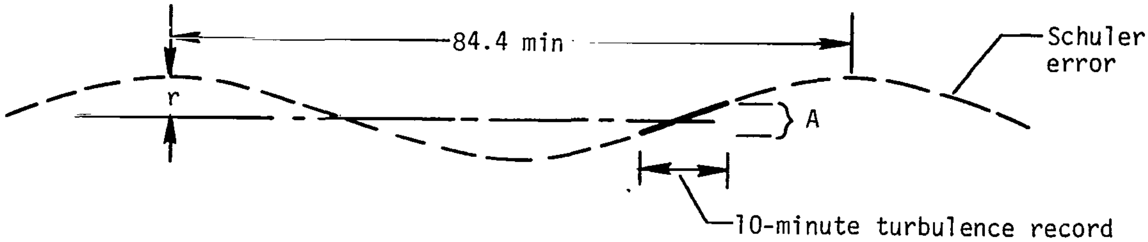

The trend can be approximated by a straight line, with the amount of "tilt" A given by

$$A = 2\left(r \sin \frac{5}{84.4} 2\pi\right) \tag{4}$$

The standard deviation σ_{trend} of a straight-line trend with zero mean, which has been digitized with closely spaced values, is

$$\sigma_{trend} = \frac{A}{\sqrt{12}} \tag{5}$$

(This σ_{trend} is used subsequently to illustrate the effect of the trend on the power spectrum.) The following table summarizes maximum possible errors estimated by the procedure outlined for various Schuler amplitudes:

Schuler amplitude, r (zero to peak)		A in 10 min (eq. (4))		Standard deviation of trend, σ_{trend} (eq. (5))	
m/sec	ft/sec	m/sec	ft/sec	m/sec	ft/sec
1.52	5.0	1.11	3.64	0.320	1.05
[a]2.29	[a]7.5	[a]1.66	[a]5.46	[a].479	[a]1.57
3.05	10.0	2.22	7.27	.640	2.10
3.81	12.5	2.77	9.09	.799	2.62

[a]Upper limit of Schuler amplitude for most flights.

These values are considered the maximum possible errors which could be present in the longitudinal and lateral turbulence time histories.

It has been observed that atmospheric turbulence is sometimes embedded in a gradually changing horizontal wind field, so that the time history has a trendlike appearance. In such cases it is impossible to determine whether a trend of the magnitude shown in the table is "noise" or real data. A simple detrending procedure applied to all time histories of longitudinal and lateral gust velocity is therefore judged to be undesirable.

Trend Effects on Power Spectra

Since the primary purpose of the MAT project is to determine power spectra which are reliable to very long wavelengths, it was desirable to determine the extent to which trend errors would affect the spectra. An artificially generated time history available from a previous study (ref. 17) was used for this purpose. Linear trends of known magnitude were added to the artificial time history, and power spectra obtained. These spectra were then compared with the spectrum of the original time history.

The results of the study are presented in figure 8. The spectrum without trend is a simulated Dryden transverse spectrum (see ref. 13) of atmospheric turbulence, with a value of L of about 180 m (600 ft). The horizontal scales have been converted to cycles/m (cycles/ft) (reciprocal of wavelength) by assuming a 190-m/sec (375-knot) true airspeed to approximate the average true airspeed of the sampling airplane. The artificial data were processed by a Fast Fourier Transform (FFT) version of the Blackman-Tukey algorithm, the method presently being used to process the flight data. The spectral window width (at the 1/2 power point) is 0.024 Hz and is approximately that required for processing 10-min data runs and maintaining 30 statistical degrees of freedom.[2]

The upper curves in figures 8(a), (b), and (c) are the spectral results obtained from the turbulence plus trend time histories when the ratios, $\sigma_{trend}/\sigma_{turbulence}$, are 0.5, 1.0, and 1.5, respectively. (The appropriate slope of the linear trend which was added to the artificial turbulence time history in each case was computed by eq. (5).) The spectral results for the turbulence alone, that is, for the time history without trend, are shown as the lower curve in each figure for comparison. The lowest frequency power estimate shown in these logarithmic plots at an inverse wavelength of about 1.64×10^{-5} cycle/m (5×10^{-6} cycle/ft) or at a wavelength of 60 960 m (200 000 ft) is actually the value computed at zero frequency and is generally discarded for actual data. Although values at zero frequency have customarily been discarded, they probably should be retained in cases where effects of trend error are known to be quite small. (The symbols in fig. 8 indicate the power estimates at the five lowest frequencies.)

For the general upper limit of the possible trend error given in the previous table (σ_{trend} = 0.479 m/sec (1.57 ft/sec)), the turbulence standard deviation

---

[2]The magnitude of the random fluctuations observed in the power spectrum obtained from the artificial time history is not directly comparable with flight data with regard to calculated statistical degrees of freedom. This is because the synthetic time history was generated by the addition of a large number of sine waves, whose amplitudes were adjusted to provide the desired spectral shape. The magnitude of the random fluctuations could be reduced to an arbitrarily low level by simply increasing the number of sine waves or by increasing the length of the time history.

would have to be as low as 0.957 m/sec (3.14 ft/sec) ($\sigma_{trend}/\sigma_{turbulence}$ = 0.5) before the effect could be as severe as that shown in figure 8(a). Similarly, if the turbulence had a standard deviation of only 0.479 m/sec (1.57 ft/sec) ($\sigma_{trend}/\sigma_{turbulence}$ = 1), the trend effect could be as severe as that depicted in figure 8(b). Figure 8(c) is generally unrealistic but might apply to one or two flights for which an extremely large Schuler error was recorded in combination with a turbulence run of very low intensity. Generally, turbulence with a standard deviation of less than about 1 m/sec (3.5 ft/sec) is considered extremely light, and unless it is very consistent, of very long duration, or of particular interest for some other reason, it would probably not be considered worth evaluating. Therefore, on the basis of figure 8, the trend would affect the power spectral estimate at the lowest nonzero frequency (15 240-m (50 000-ft) wavelength) to an appreciable extent only if the turbulence intensity is very light.

It is believed that if a narrower spectral window width were employed in the analysis, the effect of the trend would be considerably less on points adjacent to zero frequency. (The effect might be greater on the zero-frequency point, but as previously mentioned this value would probably be discarded in any event.) In the case of actual data, employing a narrower window of course requires that the time histories be longer to maintain the same statistical confidence. The use of a more rectangular shaped spectral window, available from the so-called frequency averaging algorithm (see ref. 18), should also reduce the effect of the trend considerably at the 15 240-m (50 000-ft) wavelength.

CONCLUDING REMARKS

A flight assessment has been made of a system for measuring the three components of atmospheric turbulence in the frequency range associated with airplane motions (0 to approximately 0.5 Hz). Results of the assessment indicate acceptable accuracy of resulting time histories and power spectra.

In-flight maneuvers in smooth air were used to determine residual errors in the time histories of gust velocity at the airplane short-period and Dutch-roll frequencies of approximately 0.5 and 0.25 Hz, respectively. The small errors obtained are not expected to be detectable in the power spectra. A residual error at about 0.25 Hz with amplitude of ± 0.3 to ± 0.6 m/sec (± 1 to ± 2 ft/sec) is, however, expected to be detectable in the time histories of lateral gust velocity, particularly at the higher altitudes where airplane yawing motions are large.

A data reduction procedure which effectively determines a more accurate zero for the inertial-platform vertical accelerometer and in turn removes the accompanying trend error in the airplane vertical velocity term is described. An assessment of the quantities comprising the vertical gust velocity measurements, including a comparison of the integrated vertical airplane velocity which has been trend-corrected, with pressure-derived altitude for a 12-min run, leads to the conclusion that the vertical turbulence component is essentially accurate to zero frequency. Calculations based upon the inertial-platform performance after each flight are used to indicate that maximum possible linear trend errors on the order of 1.5 to 1.8 m/sec (5 to 6 ft/sec) in 10 min could be present in the time histories of the horizontal gust velocity components. A computer experiment indicated that trends of this magnitude would affect the power spectral estimate at the lowest frequency (15 240-m (50 000-ft) wavelength) to an appreciable extent only if the turbulence intensity is very light (i.e., turbulence standard deviation (0 to 10 Hz) is about 0.9 m/sec (3 ft/sec)).

Langley Research Center
National Aeronautics and Space Administration
Hampton, VA 23665
October 15, 1976

REFERENCES

1. Houbolt, John C.: Design Manual for Vertical Gusts Based on Power Spectral Techniques. Tech. Rep. AFFDL-TR-70-106, U.S. Air Force, Dec. 1970. (Available from DDC as AD 879 736.)

2. Airplane Strength and Rigidity - Flight Loads. Mil. Specif. MIL-A-008861A(USAF), Mar. 31, 1971.

3. Pao, Yih-Ho: Spectra of Internal Waves and Turbulence in Stratified Fluids. 1. General Discussion and Indications From Measurements in Stably Stratified Atmosphere and Ocean. Radio Sci., vol. 4, no. 12, Dec. 1969, pp. 1315-1320.

4. Murrow, Harold N.; and Rhyne, Richard H.: The MAT Project - Atmospheric Turbulence Measurements With Emphasis on Long Wavelengths. Proceedings of the Sixth Conference on Aerospace and Aeronautical Meteorology of the American Meteorology Society. Nov. 1974, pp. 313-316.

5. Meissner, Charles W., Jr.: A Flight Instrumentation System for Acquisition of Atmospheric Turbulence Data. NASA TN D-8314, 1976.

6. Livingston, Sadie P.; and Gracey, William: Tables of Airspeed, Altitude, and Mach Number Based on Latest International Values for Atmospheric Properties and Physical Constants. NASA TN D-822, 1961.

7. Chilton, Robert G.: Some Measurements of Atmospheric Turbulence Obtained From Flow-Direction Vanes Mounted on an Airplane. NACA TN 3313, 1954.

8. Notess, Charles B.; and Eakin, Grady J.: Flight Test Investigation of Turbulence Spectra at Low Altitude Using a Direct Method for Measuring Gust Velocities. Rep. No. VC-839-F-1 (Contract AF 33(616)174), Cornell Aeronaut. Lab., Inc., July 1, 1954.

9. Clementson, Gerhardt C.: An Investigation of the Power Spectral Density of Atmospheric Turbulence. Ph. D. Thesis, Massachusetts Inst. Technol., 1950.

10. Crooks, Walter M.; Hoblit, Frederic M.; and Mitchell, Finic A.: Project HICAT - High Altitude Clear Air Turbulence Measurements and Meteorological Correlations. AFFDL-TR-68-127, Vol. I, U.S. Air Force, Nov. 1968. (Available from DDC as AD 846 086.)

11. Jones, J. W.; Mielke, R. H.; Jones, G. W.; et al.: Low Altitude Atmospheric Turbulence LO-LOCAT Phase III. Volume I, Part I, Data Analysis. AFFDL-TR-70-10, Vol. I, Pt. I, U.S. Air Force, Nov. 1970. (Available from DDC as AD 878 776.)

12. Rhyne, Richard H.; and Steiner, Roy: Power Spectral Measurement of Atmospheric Turbulence in Severe Storms and Cumulus Clouds. NASA TN D-2469, 1964.

13. Houbolt, John C.; Steiner, Roy; and Pratt, Kermit G.: Dynamic Response of Airplanes to Atmospheric Turbulence Including Flight Data on Input and Response. NASA TR R-199, 1964.

14. Crooks, Walter M.; Hoblit, Frederic M.; Prophet, David T.; et al.: Project HICAT - An Investigation of High Altitude Clear Air Turbulence. AFFDL-TR-67-123, Vol. I, U.S. Air Force, Nov. 1967. (Available from DDC as AD 824 865.)

15. Margason, Richard J.; and Lamar, John E.: Vortex-Lattice FORTRAN Program for Estimating Subsonic Aerodynamic Characteristics of Complex Planforms. NASA TN D-6142, 1971.

16. Draper, Charles S.; Wrigley, Walter; and Hovorka, John: Inertial Guidance. Pergamon Press, 1960.

17. Keisler, Samuel R.; and Rhyne, Richard H.: An Assessment of Prewhitening in Estimating Power Spectra of Atmospheric Turbulence at Long Wavelengths. NASA TN D-8288, 1976.

18. Otnes, Robert K.; and Enochson, Loren: Digital Time Series Analysis. John Wiley and Sons Inc., c.1972.

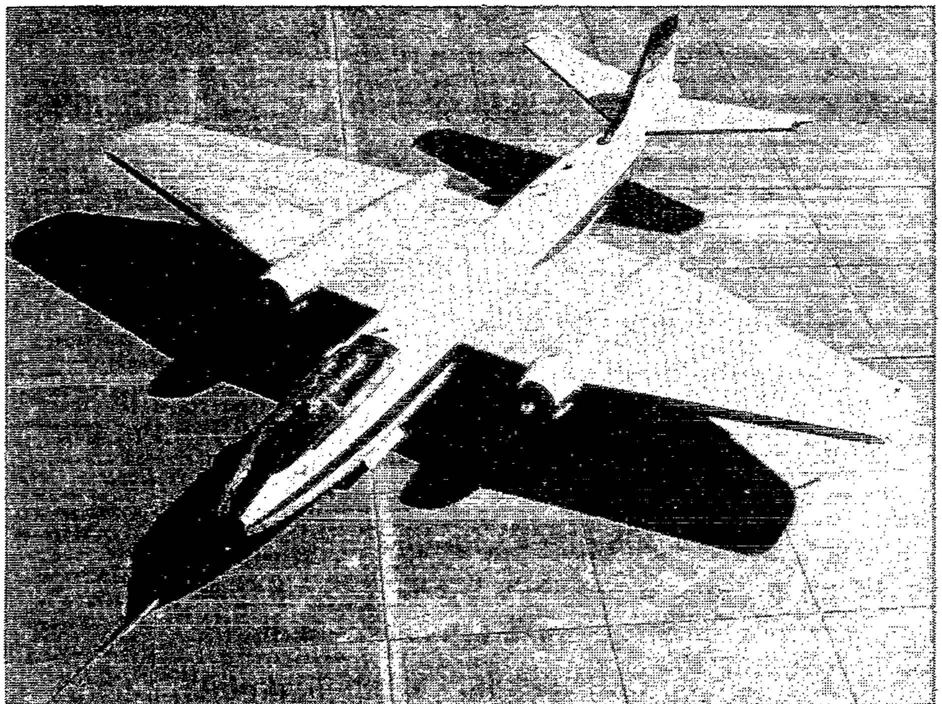

L-74-5992

Figure 1.- Photograph of MAT project airplane with nose-boom installation.

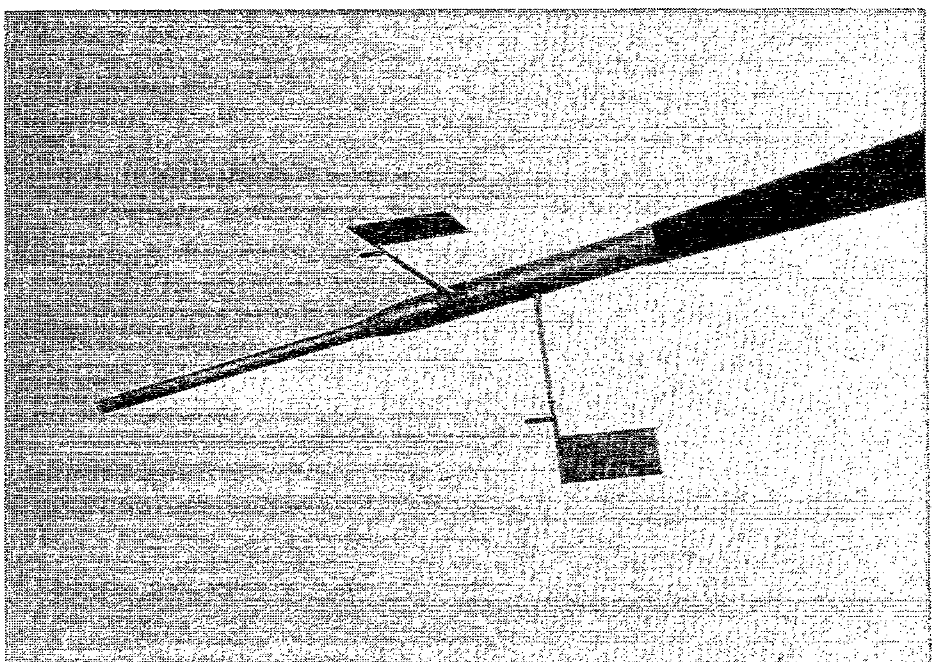

L-74-6000

Figure 2.- Pitot-static head and balsa flow-direction vanes installed on nose boom.

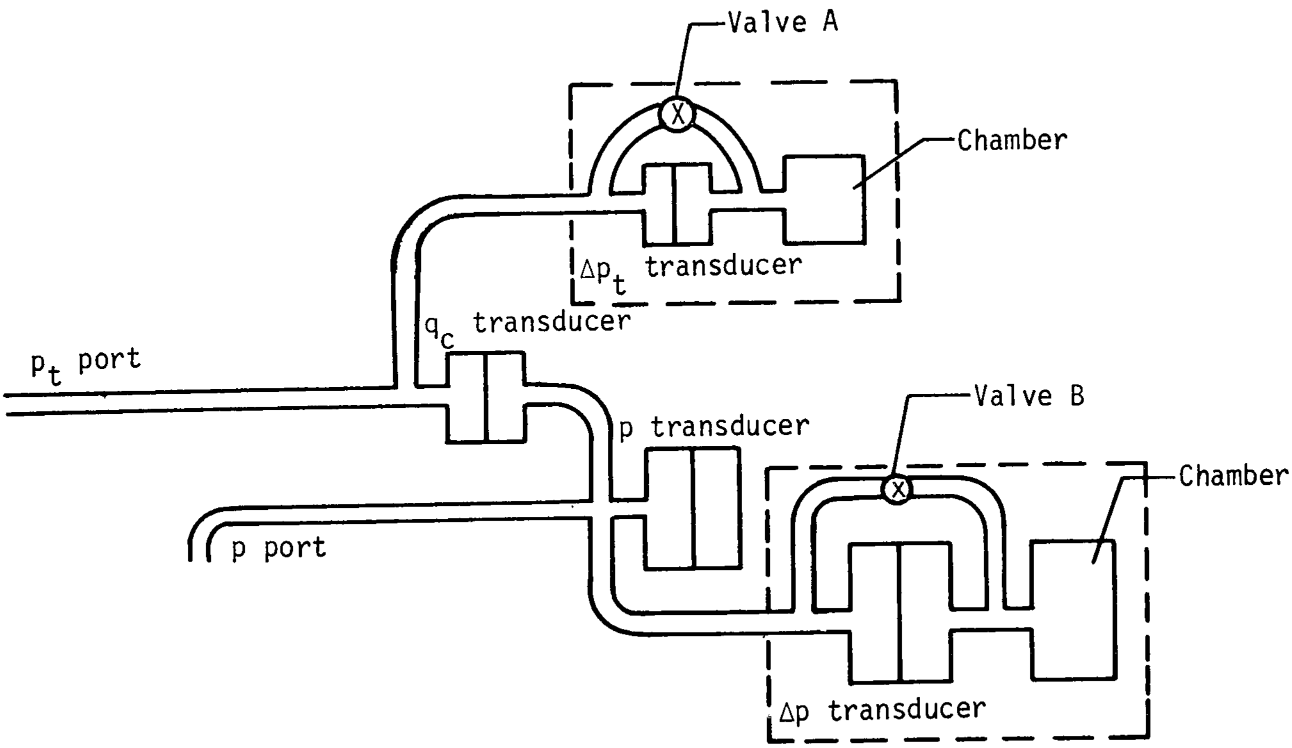

Figure 3.- Schematic of special pressure-measuring system for obtaining longitudinal turbulence component.

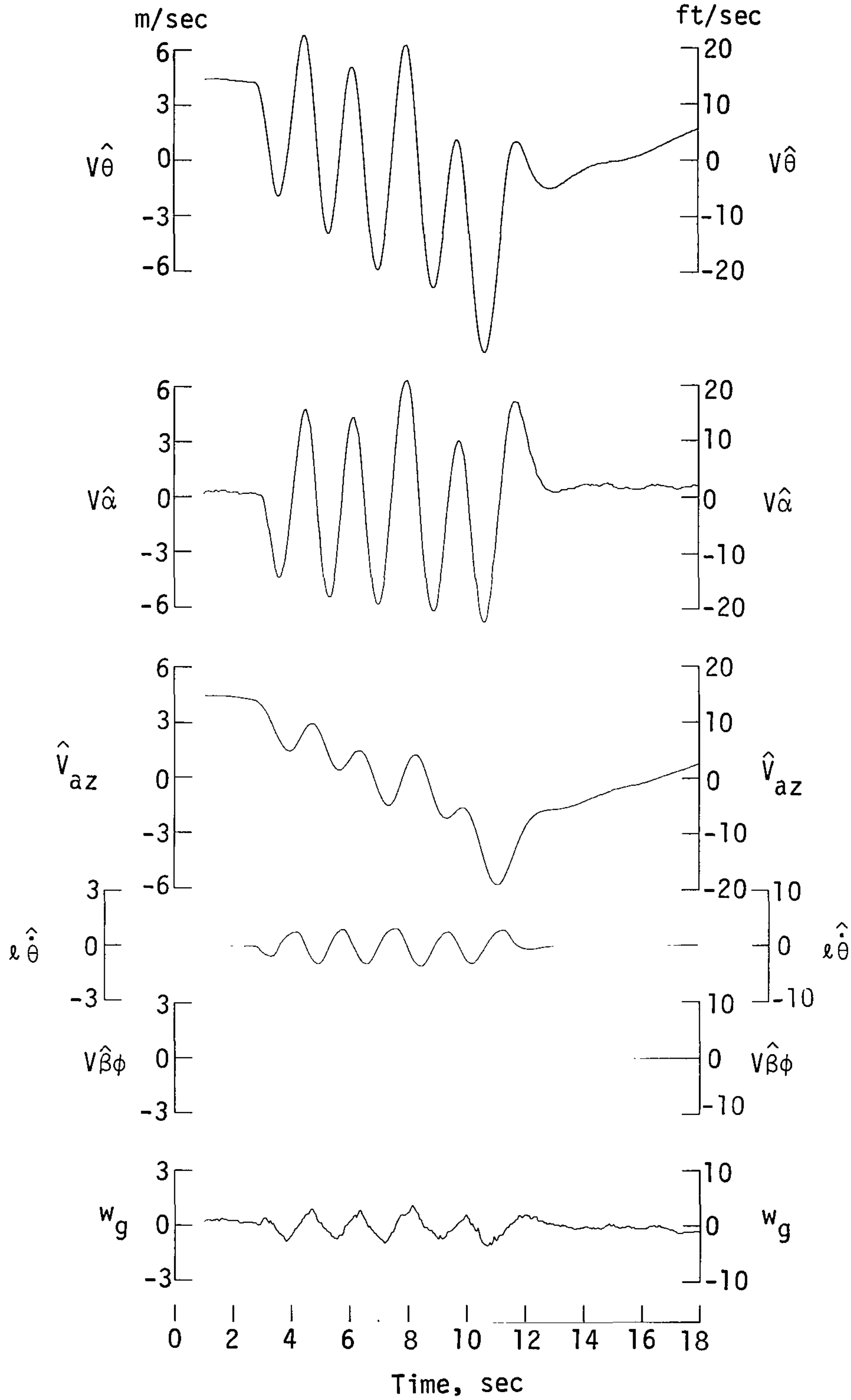

Figure 4.- Pitching oscillation in smooth air. Altitude, 7990 m (26 200 ft).

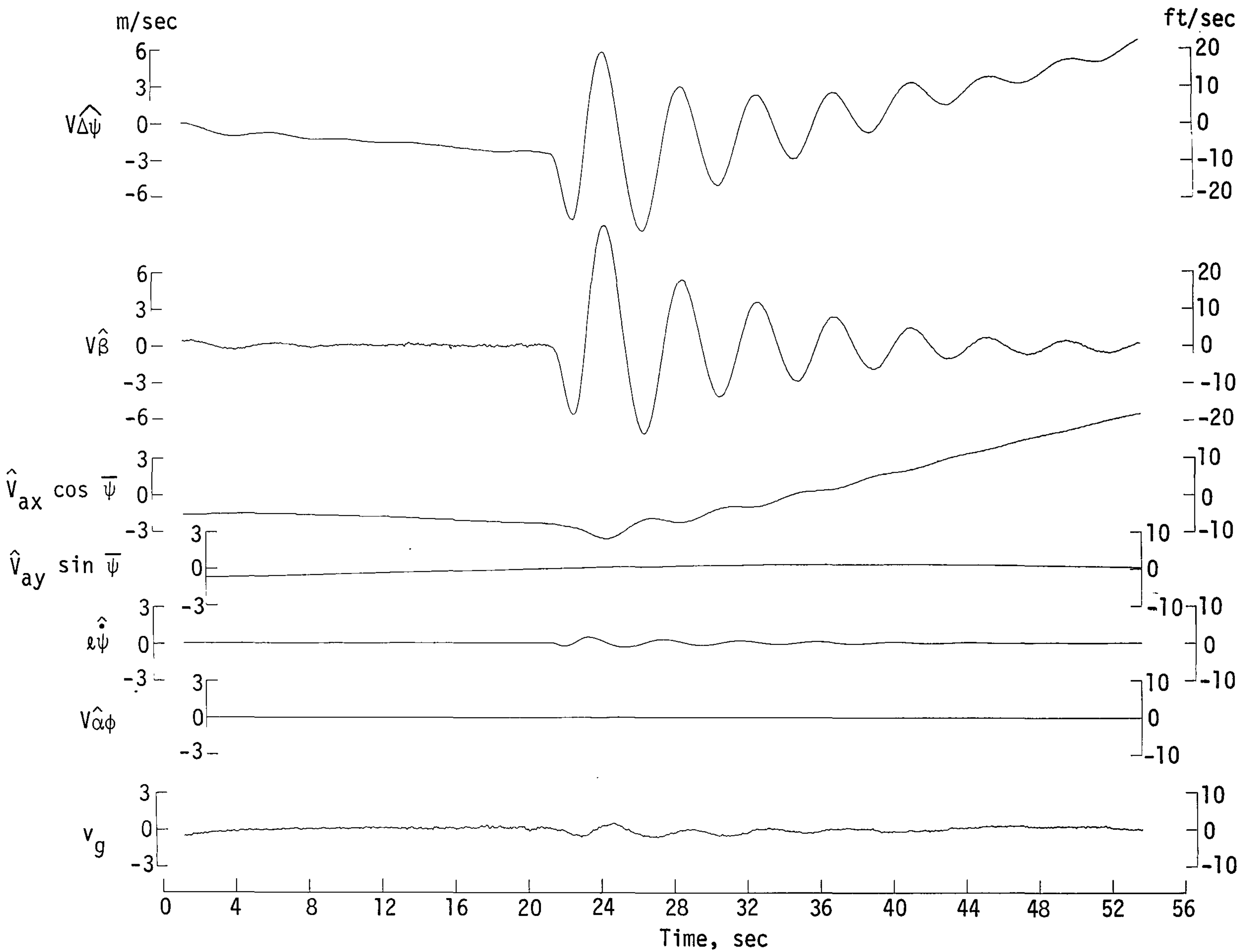

Figure 5.- Yawing oscillation in smooth air. Altitude, 4660 m (15 300 ft).

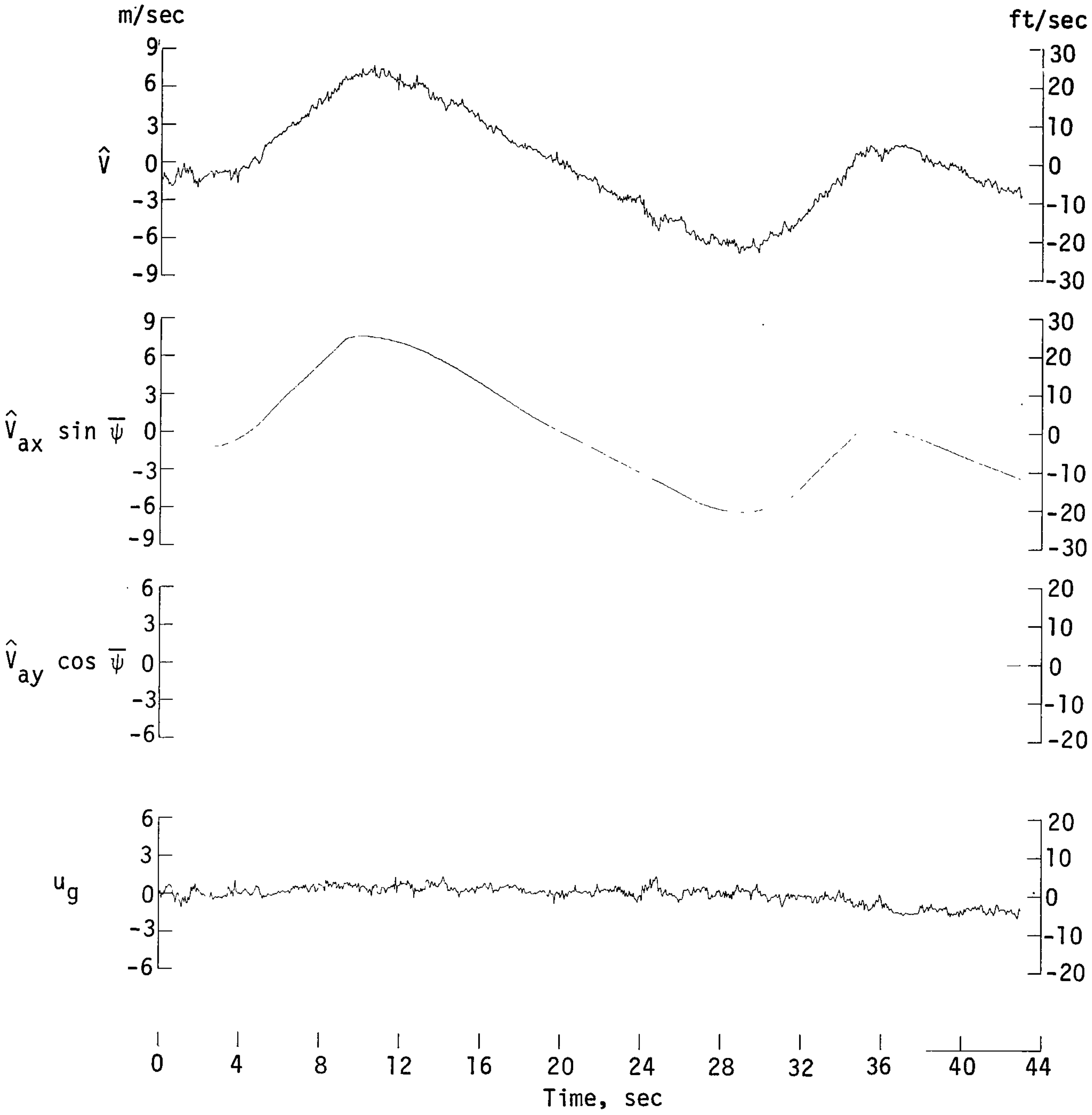

Figure 6.- Speed-change maneuver in very slight turbulence. Altitude, 4480 m (14 700 ft).

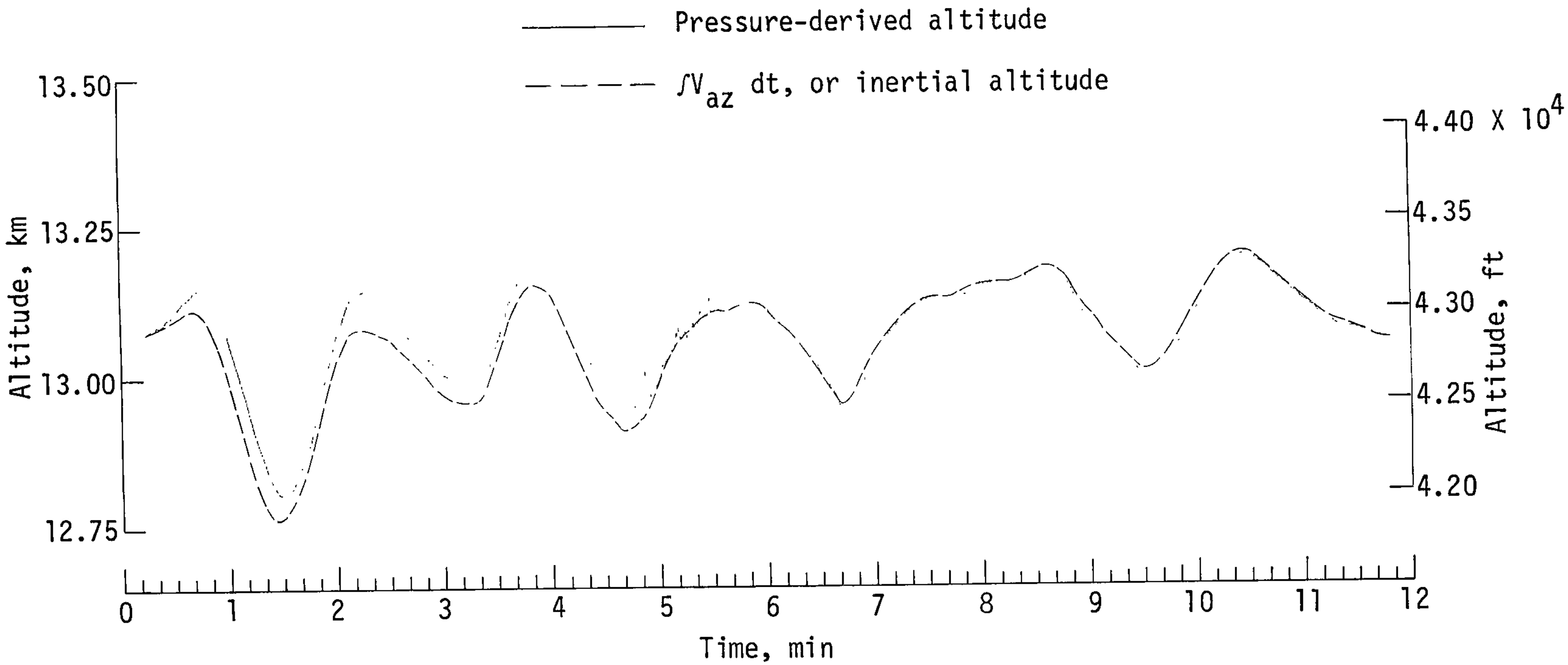

Figure 7.- Time histories of integral of vertical airplane velocity and pressure-derived altitude in a 12-min wind-shear turbulence run.

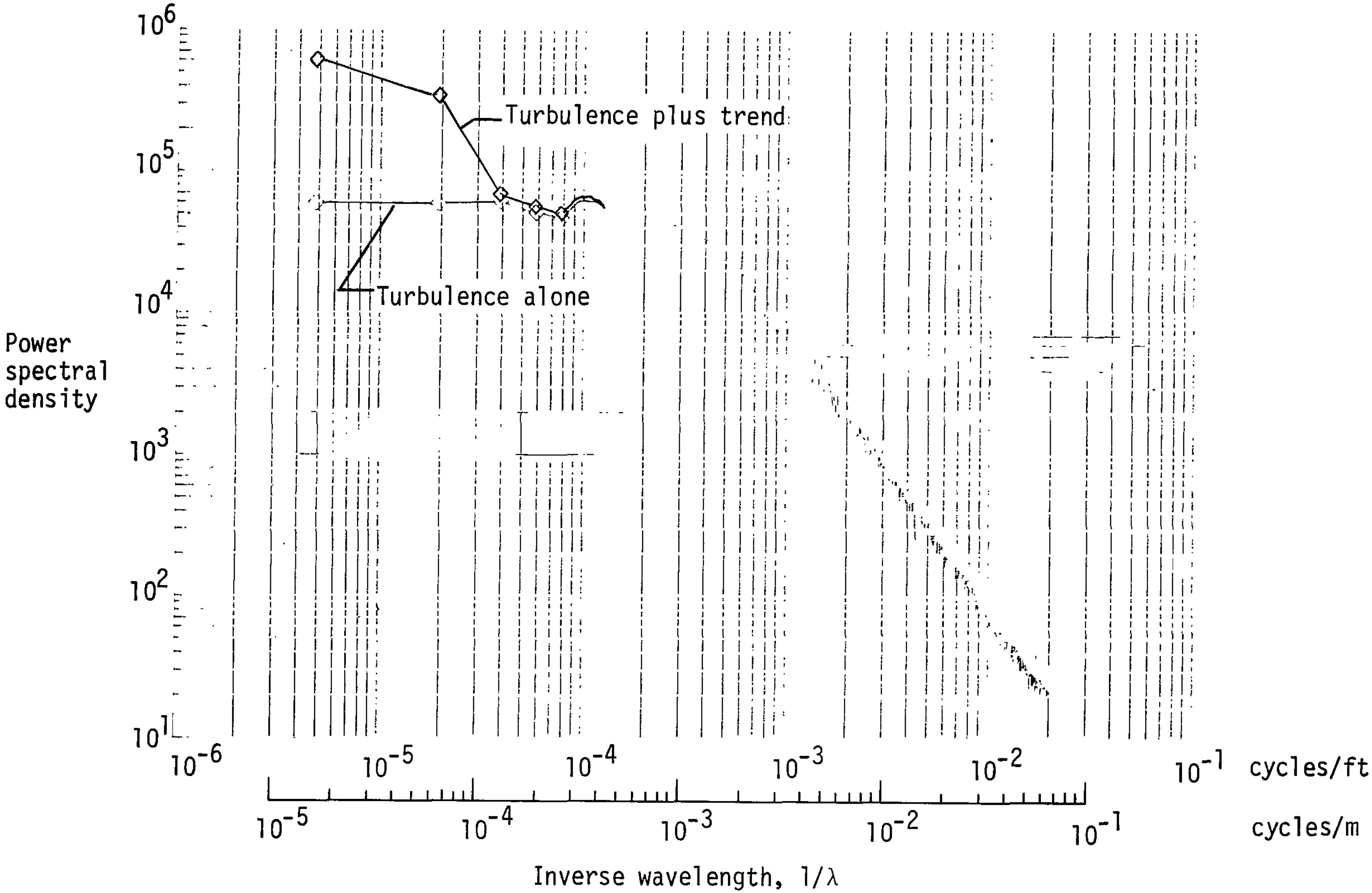

(a) $\sigma_{trend}/\sigma_{turbulence} = 0.5.$

Figure 8.- Linear trend effect on power spectrum of artificially generated time history. (Symbols denote power spectral estimates at five lowest frequencies.)

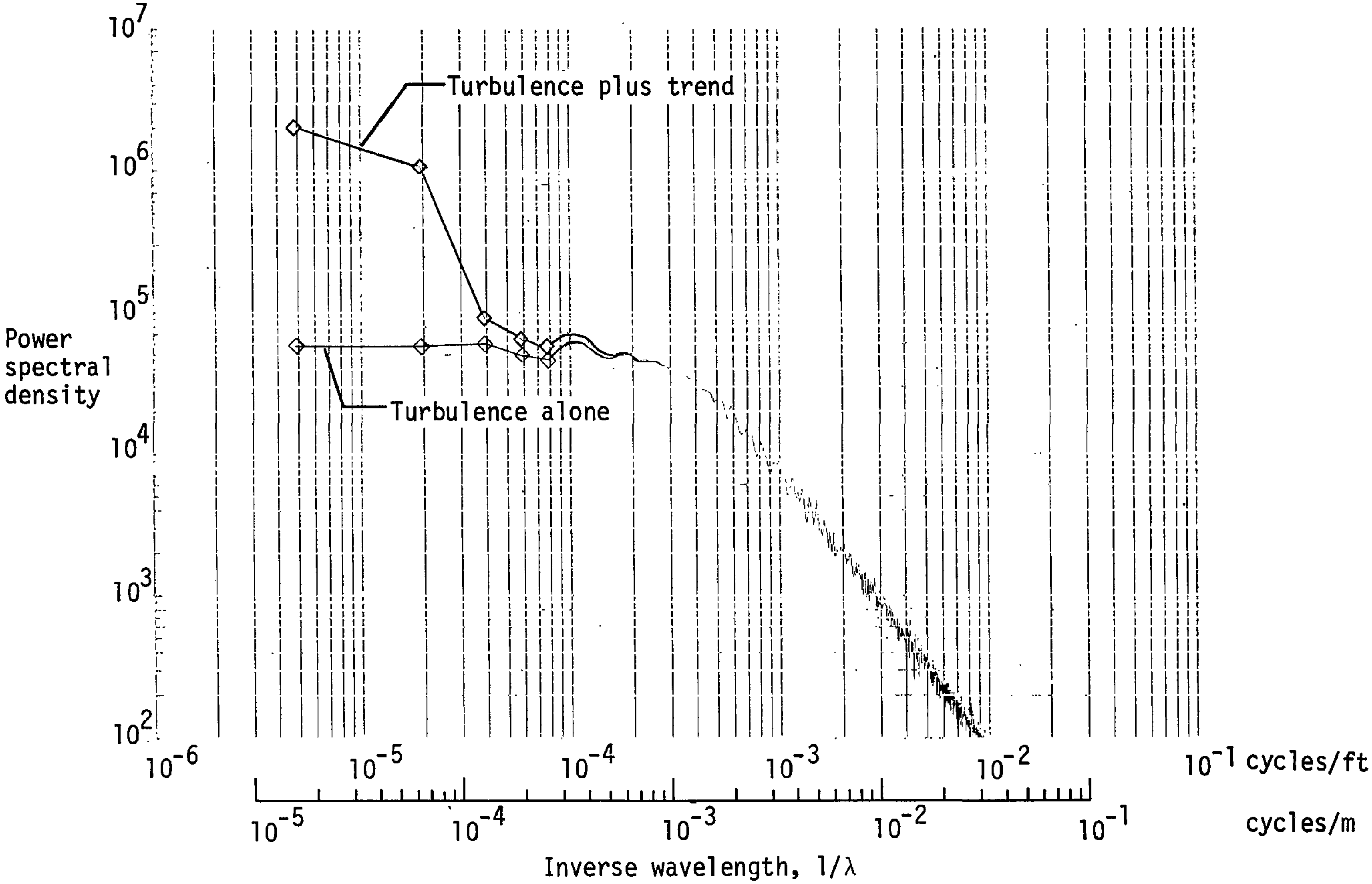

(b) $\sigma_{trend}/\sigma_{turbulence} = 1.0.$

Figure 8.- Continued.

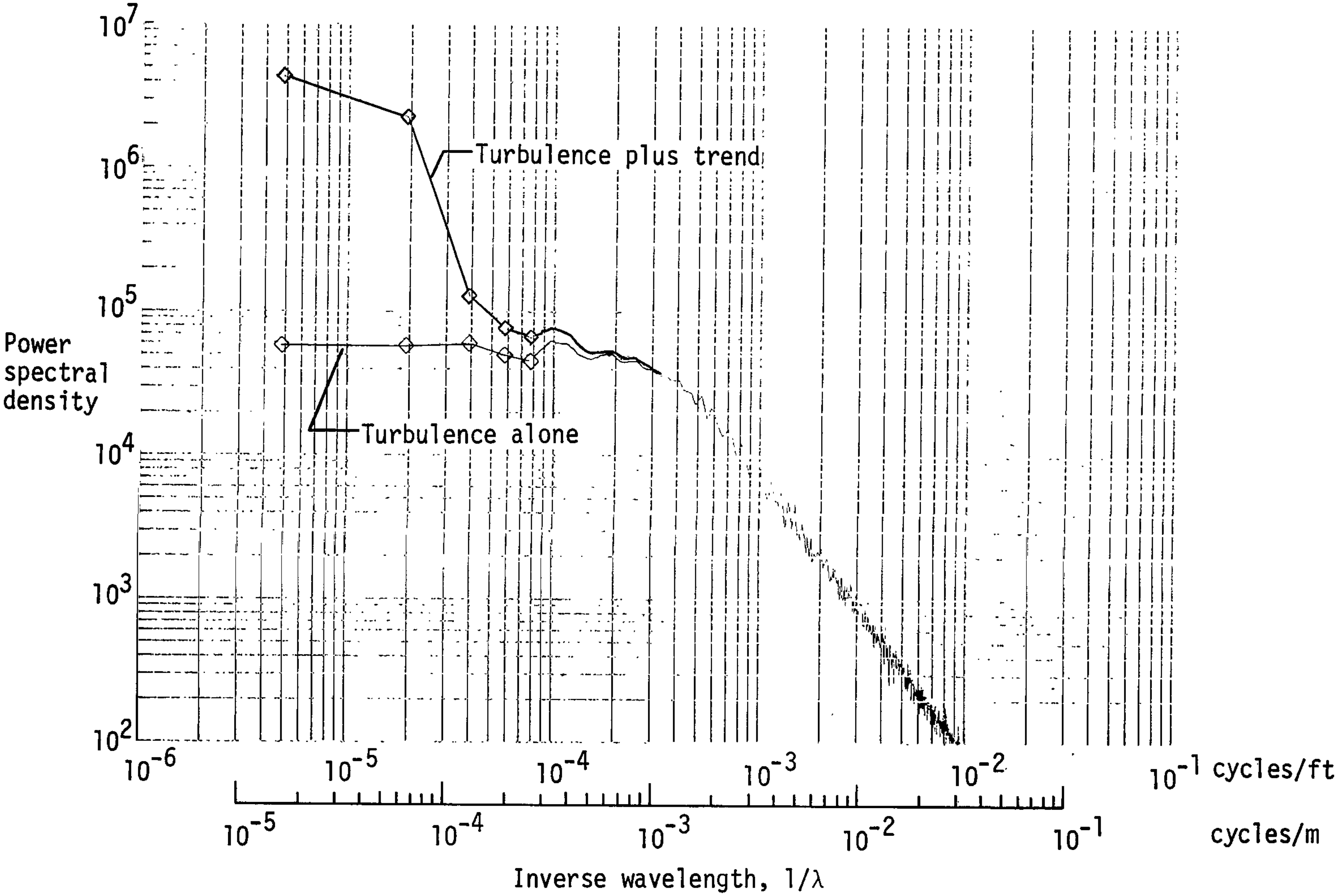

(c) $\sigma_{trend}/\sigma_{turbulence} = 1.5$.

Figure 8.- Concluded.

NASA-Langley, 1976 L-10888

"The aeronautical and space activities of the United States shall be conducted so as to contribute . . . to the expansion of human knowledge of phenomena in the atmosphere and space. The Administration shall provide for the widest practicable and appropriate dissemination of information concerning its activities and the results thereof."

—NATIONAL AERONAUTICS AND SPACE ACT OF 1958

NASA SCIENTIFIC AND TECHNICAL PUBLICATIONS

TECHNICAL REPORTS: Scientific and technical information considered important, complete, and a lasting contribution to existing knowledge.

TECHNICAL NOTES: Information less broad in scope but nevertheless of importance as a contribution to existing knowledge.

TECHNICAL MEMORANDUMS: Information receiving limited distribution because of preliminary data, security classification, or other reasons. Also includes conference proceedings with either limited or unlimited distribution.

CONTRACTOR REPORTS: Scientific and technical information generated under a NASA contract or grant and considered an important contribution to existing knowledge.

TECHNICAL TRANSLATIONS: Information published in a foreign language considered to merit NASA distribution in English.

SPECIAL PUBLICATIONS: Information derived from or of value to NASA activities. Publications include final reports of major projects, monographs, data compilations, handbooks, sourcebooks, and special bibliographies.

TECHNOLOGY UTILIZATION PUBLICATIONS: Information on technology used by NASA that may be of particular interest in commercial and other non-aerospace applications. Publications include Tech Briefs, Technology Utilization Reports and Technology Surveys.

Details on the availability of these publications may be obtained from:

SCIENTIFIC AND TECHNICAL INFORMATION OFFICE

NATIONAL AERONAUTICS AND SPACE ADMINISTRATION

Washington, D.C. 20546